Supporting Information

$[Pb_3Cu_2I_{10}(phen)_4]_n$: A novel organic-inorganic hybrid ferromagnetic semiconductor

Le-Qing Fan,*[ab] Xin Jin,[a] Dong-Xu Li,[a] Chong-Bin Tian[b] and Ji-Huai Wu[a]

[a] *Engineering Research Center of Environment-Friendly Functional Materials, Ministry of Education, College of Materials Science and Engineering, Huaqiao University, Xiamen, Fujian 361021, China.*

[b] *State Key Laboratory of Structural Chemistry, Fujian Institute of Research on the Structure of Matter, Chinese Academy of Sciences, Fuzhou, Fujian 350002, China*.

*Corresponding author. E-mail: leqingfan@163.com

Experimental Section:

X-Ray Crystallography. The crystallographic data for **1** were collected on a Rigaku Mercury CCD area-detector equipped with a graphite-monochromated Mo$K\alpha$ radiation (λ = 0.71073 Å) at 293(2) K using an ω-2θ scan mode. Absorption corrections were performed by the CrystalClear program. The structure were solved by direct methods using SHELXS-97 program and refined by full-matrix least-squares refinement on F^2 with the aid of SHELXL-97 program. All non-hydrogen atoms were refined anisotropically. Hydrogen atoms attached to carbon were placed in geometrically idealized positions and refined using a riding model. Crystallographic data for the structure reported in this paper have been deposited with the Cambridge Crystallographic Data Centre as supplementary publication no. CCDC 1507207. Copy of the data can be obtained free of charge on application to CCDC, 12 Union Road, Cambridge CB2 1EZ, UK (fax: +44 1223 336-033; e-mail: deposit@ccdc.cam.ac.uk).

Some refinement details and crystal data of **1** are summarized in Table S4. Selected bond lengths and angles of **1** are shown in Table S1.

Materials and Physical Measurements. All chemicals and solvents were commercially purchased and used without further purification. Powder X-ray diffraction data were collected on a Bruker D8 Advance diffractometer. Elemental analyses were measured on a Vario EL III element analyzer. Magnetic testes were carried out with a PPMS-9T magnetometer. A diamagnetic correction was estimated from Pascal's constants. The temperature dependence of the magnetic susceptibilities was investigated over the temperature range of 2–300 K under a magnetic field of 1 kOe. Diffuse reflectance spectra were recorded at room temperature on a PerkinElmer Lambda 950 UV-vis spectrometer equipped with an integrating sphere with the $BaSO_4$ plate as the reference. The absorption data are calculated from the Kubelka-Munk function, $F(R) = (1 - R)^2/2R$, where R is the experimentally observed reflectance. Because **1** and PbI_2 have a direct band, their optical band gaps are calculated by $F(R)^2$ vs. photon energy plots. The band gap is determined as the intersection point of the energy axis with the extrapolated linear portion of the absorption edge.

Computational Descriptions. The crystallographic data of **1** and binary PbI_2 (ICSD-24262) were used to calculate electronic band structures and density of states (DOS) by the CASTEP code. This code uses a plane-wave basis set with Vanderbilt ultrasoft pseudopotentials to approximate the interactions between core and valence electrons. The exchange-correlation energy was calculated through the Perdew-Burke-Ernzerhof (PBE) modification to the generalized gradient approximation (GGA). The kinetic energy cutoff we used is 280 eV. Pseudo atomic calculations were carried out for Pb $5d^{10}6s^26p^2$, Cu $3d^{10}4s^1$, I $5s^25p^5$, N $2s^22p^3$, C $2s^22p^2$ and H $1s^1$. The smearing width for the DOS is 0.05 eV. The other calculating parameters and convergent criteria were set by the default values of the CASTEP code.

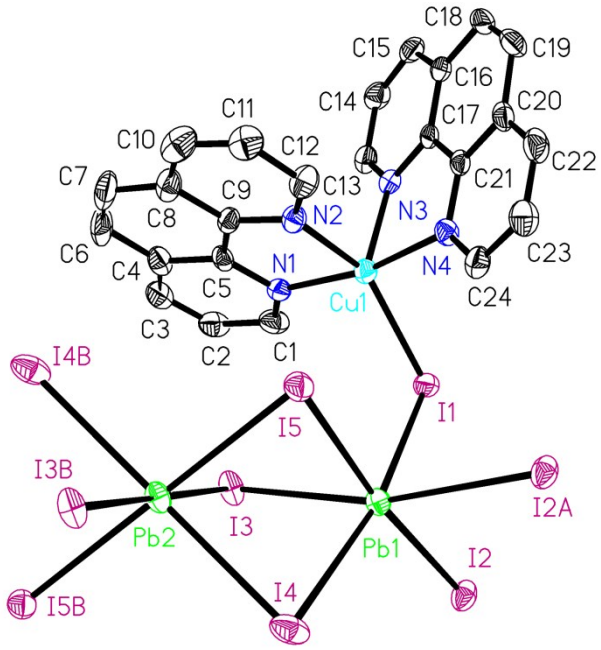

Fig. S1 ORTEP plot of the asymmetric unit of **1** (30% probability ellipsoids). All H atoms are omitted for clarity. Symmetry codes: (A) $-x + 1, -y + 2, -z + 1$; (B) $-x + 2, -y + 2, -z + 1$.

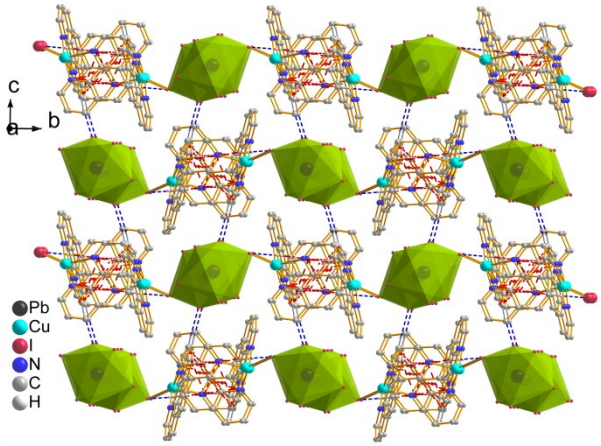

Fig. S2 Packing diagram of **1** viewed approximately down the [100] direction. Some H atoms are omitted for clarity. The aromatic π–π stacking interactions and hydrogen-bonding interactions are shown in red and blue broken lines, respectively.

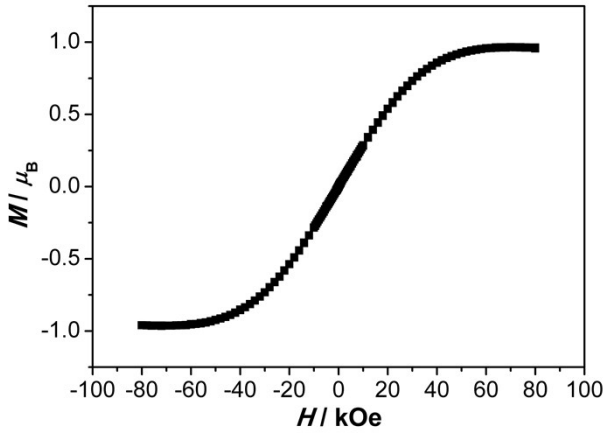

Fig. S3 Magnetization vs. field at 2 K for **1**.

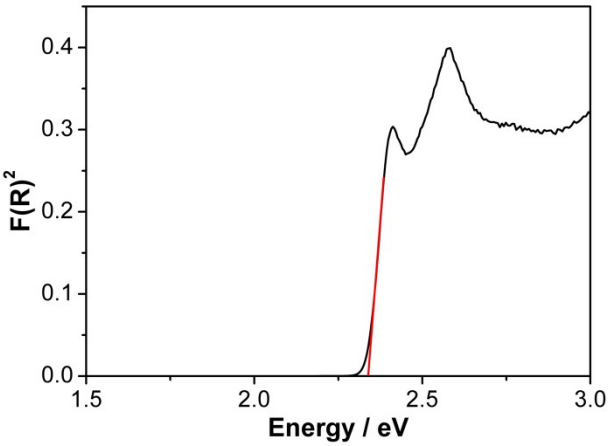

Fig. S4 Plot of $F(R)^2$ vs. photon energy for PbI_2.

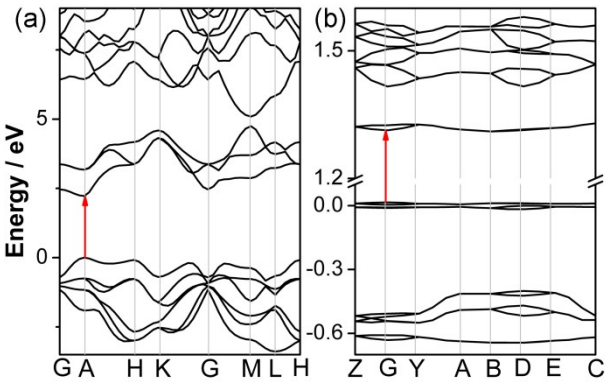

Fig. S5 Band structures of (a) **1** and (b) PbI_2.

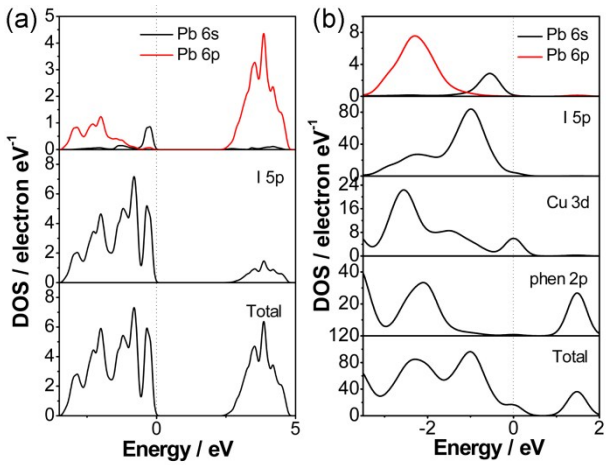

Fig. S6 Total and partial DOS plots of (a) **1** and (b) PbI_2. The Fermi level is set at 0 eV.

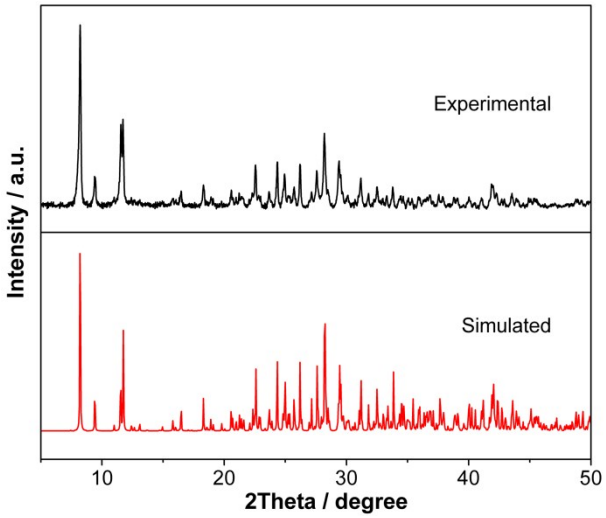

Fig. S7 Experimental and simulated X-ray powder diffraction patterns of **1**.

Table S1 Selected bond lengths (Å) and angles (°) for **1**.

Pb(1)–I(1)	3.2132(6)	Pb(2)–I(4)#2	3.3161(6)
Pb(1)–I(2)	3.2326(6)	Pb(2)–I(5)	3.2580(5)
Pb(1)–I(2)#1	3.2981(6)	Pb(2)–I(5)#2	3.2580(5)
Pb(1)–I(3)	3.2114(6)	Cu(1)–I(1)	2.5980(9)
Pb(1)–I(4)	3.2414(6)	Cu(1)–N(1)	1.992(6)
Pb(1)–I(5)	3.2300(6)	Cu(1)–N(2)	2.098(5)
Pb(2)–I(3)	3.1739(5)	Cu(1)–N(3)	2.158(5)
Pb(2)–I(3)#2	3.1739(5)	Cu(1)–N(4)	1.995(5)
Pb(2)–I(4)	3.3161(6)		
I(3)–Pb(1)–I(1)	83.837(15)	I(5)–Pb(2)–I(5)#2	180.000(15)
I(3)–Pb(1)–I(5)	83.433(15)	I(3)#2–Pb(2)–I(4)	96.659(14)
I(1)–Pb(1)–I(5)	96.330(15)	I(3)–Pb(2)–I(4)	83.341(14)
I(3)–Pb(1)–I(2)	100.417(15)	I(5)–Pb(2)–I(4)	80.657(14)
I(1)–Pb(1)–I(2)	79.592(15)	I(5)#2–Pb(2)–I(4)	99.343(14)
I(5)–Pb(1)–I(2)	173.980(17)	I(3)#2–Pb(2)–I(4)#2	83.341(14)
I(3)–Pb(1)–I(4)	83.959(15)	I(3)–Pb(2)–I(4)#2	96.659(14)
I(1)–Pb(1)–I(4)	167.796(17)	I(5)–Pb(2)–I(4)#2	99.343(14)
I(5)–Pb(1)–I(4)	82.215(16)	I(5)#2–Pb(2)–I(4)#2	80.657(14)
I(2)–Pb(1)–I(4)	102.709(18)	I(4)–Pb(2)–I(4)#2	180.0
I(3)–Pb(1)–I(2)#1	165.820(17)	N(1)–Cu(1)–N(4)	167.9(2)
I(1)–Pb(1)–I(2)#1	84.235(16)	N(1)–Cu(1)–N(2)	81.3(2)
I(5)–Pb(1)–I(2)#1	90.293(14)	N(4)–Cu(1)–N(2)	88.4(2)
I(2)–Pb(1)–I(2)#1	84.914(14)	N(1)–Cu(1)–N(3)	94.5(2)
I(4)–Pb(1)–I(2)#1	107.847(16)	N(4)–Cu(1)–N(3)	80.1(2)
I(3)#2–Pb(2)–I(3)	180.0	N(2)–Cu(1)–N(3)	95.6(2)
I(3)#2–Pb(2)–I(5)	96.427(13)	N(1)–Cu(1)–I(1)	96.21(16)
I(3)–Pb(2)–I(5)	83.573(13)	N(4)–Cu(1)–I(1)	95.87(17)
I(3)#2–Pb(2)–I(5)#2	83.573(13)	N(2)–Cu(1)–I(1)	146.90(16)

I(3)–Pb(2)–I(5)#2	96.427(12)	N(3)–Cu(1)–I(1)	117.49(14)

Symmetry transformations used to generate equivalent atoms: #1 –*x* + 1, –*y* + 2, –*z* + 1; #2 –*x* + 2, –*y* + 2, –*z* + 1.

Table S2 π–π stacking interaction parameters for **1**.

R(I) ···*R*(J)	Cg–Cg (Å)	Alpha (°)	*R*(I)_Perp (Å)
R(1)···*R*(1)#2	4.397(5)	0.02	3.583
R(1)···*R*(4) #2	4.139(5)	0.30	3.574
R(2)···*R*(3)#1	3.616(4)	2.22	3.418
R(2)···*R*(5)#1	3.693(4)	1.71	3.423
R(3)···*R*(2)#1	3.615(4)	2.22	3.377
R(3)···*R*(5)#1	4.402(4)	0.99	3.414
R(4)···*R*(1)#2	4.140(5)	0.30	3.581
R(5)···*R*(2)#1	3.693(4)	1.71	3.456
R(5)···*R*(3)#1	4.403(4)	0.99	3.460
R(5)···*R*(5)#1	3.811(4)	0.03	3.424

R(1), *R*(2), *R*(3), *R*(4) and *R*(5) represent the pyridine rings N2/C8-C12, N3/C13-C17, N4/C20-24, C4-C9 and C16-C21, respectively. Cg–Cg is the distance between ring centroids. Alpha is the dihedral angle between rings I and J. *R*(I)_Perp is the perpendicular distance of *R*(I) on *R*(J). Symmetry transformations used to generate equivalent atoms: #1 –*x* + 1, –*y* + 2, –*z* + 1; #2 –*x* + 2, –*y* + 2, –*z* + 1.

Table S3 Hydrogen bond distances (Å) and angles (°) for **1**.

D–H···A	*d*(D–H)	*d*(H···A)	*d*(D–A)	∠(DHA)
C(18)–H(18A)···I(1)#1	0.93	3.00	3.676(8)	131
C(11)–H(11A)···I(3)#2	0.93	3.00	3.765(9)	140

Symmetry transformations used to generate equivalent atoms: #1 –*x* + 1, –*y* + 1, –*z* + 1; #2 *x* + 1/2, –*y* + 3/2, *z* + 1/2.

Table S4 Crystallographic data and structure refinement parameters for **1**.

Empirical formula	$C_{48}H_{32}Cu_2I_{10}N_8Pb_3$
Formula weight	2738.47
Color and habit	Black, prism
Crystal size (mm)	0.20 × 0.20 × 0.06
Crystal system	Monoclinic
Space group	$P2_1/n$
a (Å)	13.0188(6)
b (Å)	15.3408(6)
c (Å)	16.2776(7)
β (°)	112.263(5)
V (Å^3)	3008.6(2)
Z	2
T (K)	293(2)
Density, calculated (g cm^{-3})	3.023
Absorption coefficient (mm^{-1})	14.232
F(000)	2420
λ (Å)	0.71073
h, k, and l range	–17 to 17, –20 to 19, –22 to 21
Reflections measured	20210
Independent reflections	7123 [R(int) = 0.0355]
Refinement method	Full-matrix least-squares on F^2
θ range for data collection (°)	2.70 to 29.21
Goodness-of-fit on F^2	1.063
Final R indices [$I > 2\sigma(I)$][a]	R_1 = 0.0377, wR_2 = 0.0716
R indices (all data)[a]	R_1 = 0.0546, wR_2 = 0.0778
Largest difference peak and hole (e Å^{-3})	1.302 and –1.024

[a] $R_1 = \Sigma||F_0| - |F_c||/\Sigma|F_0|$, w$R_2 = [\Sigma w(|F_0^2| - |F_c^2|)^2/\Sigma w(F_0^2)^2]^{1/2}$